E144: Backgrounds to nonlinear Compton measurements in Ecal - experimental status

Konstantin Shmakov
(January 23, 1997)

List of Tables

List of Figures

I. DIFFERENT SOURCES OF THE BACKGROUND

Electrons originating from Nonlinear Compton processes are bent by the spectrometer magnet and detected by the electromagnetic calorimeter (Ecal). At the same time electrons from ordinary N=1 Compton scattering are also bent by the spectrometer magnet through smaller angle (due to higher energy) and pass above the Ecal. Recall that nonlinear Compton signal from N=2,3,4 interactions measured by Ecal is in the range $10^2 - 10^4$ GeV. At the same time the flux of ordinary N=1 Compton electrons is of the order of $10^6 - 10^8$ GeV. These electrons leave the vacuum chamber and pass through several materials where even a small fraction of this flux scattered into Ecal could complicate the measurement of the nonlinear Compton signal. Three sources of such background were identified:

1. Fe window of the vacuum chamber. Though the thickness of the window is small (9mm) the location of the window in front of Ecal allows N=1 electrons scattered through a relatively small angle of $10 - 30°$ to reach Ecal. This background dominates in the front longitudinal section of Ecal.

2. Beam pipe on top of Ecal. Part of N=1 electron flux strikes walls of the beam pipe (1/16" thick) at a very small angle $\approx 1°$. This increases the probability of electrons scattering in the beam pipe at large angles $\approx 90°$. Because this background originates above Ecal it has most effect in the top row.

3. N=1 electrons exit the beam pipe and hit flanges of the beam pipe and other materials behind Ecal. Splash-back from those electrons (albedo) reaches Ecal causing background mainly in the rear longitudinal section.

Note that changes in the design of the beam pipe and vacuum chamber window made prior to August 96 run reduced backgrounds from sources 1) and 2) to a level more than an order of magnitude smaller than the signal. Background from the 3-rd source (splash-back) is reduced by Pb-brick shielding behind Ecal. Finally the last segment of the Ecal ($\approx 4X_0$) was not used in the analysis and hence serves as additional shielding.

Backgrounds which are uniformly distributed in the transverse direction (perpendicular to the beam pipe) can be effectively subtracted from the signal due to the design of the Calorimeter and readout scheme. In each longitudinal segment Ecal has 4 readout segments in the transverse direction - 2 central and 2 outer pads which are readout separately. Electrons from the nonlinear Compton processes are deflected vertically along the center line of Ecal and develop electromagnetic showers in 2 central pads with about 10 % of those showers leaking to the outer pads. Hence subtraction of the signal in the outer pads from that in the central pads (taking into account the shower leakage) can eliminate uniform background in the central pads even if they exceed the signal level.

The difficulty for reconstruction of the nonlinear Compton signal is in the nonuniform component of the background in the transverse direction. Monte Carlo studies of the detectors helped to identify main sources of this nonuniform background and to define the strategy to reduce it. Nonuniform component in the background is primarily due to the scattering in front of Ecal (source 1) and on top of Ecal (source 2). Albedo from the back (source 3) is almost uniform and the subtraction of outer pads background almost completely eliminates this background. This result is confirmed by direct measurements.

II. DETERMINATION OF BACKGROUNDS

Measurement of backgrounds are made when only N=1 Compton scattering occurs at the electron-laser interaction without higher order processes. This condition can be achieved by defocusing laser beam to increase the area of the laser focus with low maximum laser intensity. However since in E144 it was not possible to change the area of the laser focus an alternative method of effectively "defocusing" the laser beam was used. Due to 17° crossing angle between electron and laser beams it was possible to move laser focus outside the electron beam in the horizontal X-direction perpendicular to the electron beam and still have collisions by adjusting the relative timing of the electron and laser beams. A typical two dimensional X-T scan is shown in Fig. 1. The signal during X-T scan is measured by two detectors - one detector (CCM1 or EC31) is used to measure the rate of N=1 Compton processes and one detector (ECAL) to measure the rate of nonlinear (N=2) processes. When the laser focus is inside the electron beam one sees the clear signal in N=2 detector as well as in N=1 detector. With the laser focus outside the electron beam there are no nonlinear processes while the N=1 rate is still high (N=1 rate depends only on laser energy)

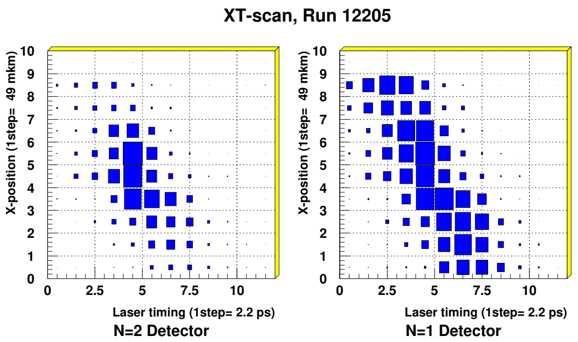

FIG. 1. Example of XT-scan (run 12205) for IR circular polarized laser. Horizontal axis - timing of the laser (ps), vertical - X-position of the laser IP box (μm). Area of the boxes is proportional to the signal. Two detectors are shown - Ecal in the position where it measures N=2 signal and N=1 gamma counter (CCM1). The slope of N=1 signal is due to 17° crossing angle between electron and laser beams

The slope of N=1 constant rate on X-T plot corresponds to 17° crossing angle between the electron and laser beams. From geometrical consideration the relation between Δx and Δt is:

$$\Delta x \left(\frac{1}{\sin\alpha} + \frac{1}{\tan\alpha} \right) = c\Delta t$$

where $\alpha = 17°$ is the crossing angle. Because $c = 299.8\,\mu m/ps$ we find that the expected slope is:

$$\Delta x\,[\mu m] \;=\; 44.80\,\Delta t\,[ps]$$

X-T scans were made frequently during the data taking to monitor and adjust the position and the timing of the laser. They were taken with different Ecal positions and different laser intensities.

To find backgrounds in Ecal caused by re-scattering of N=1 electrons one can look at the asymptotic behavior of the Ecal signal (plotted versus X, or T or constant N=1 line) for center and outer pads while the laser focus is outside the electron beam. Higher order processes should not contribute to the measurements when the laser focus is completely outside the electron beam and the only source of the signal is then the background from N=1 processes. By normalizing Ecal signal to the N=1 gamma flux (measured by CCM1 or EC37) one can expect this signal to go asymptotically to some constant levels presumably different for center and outer pads of Ecal.

By fitting these distributions by the Gaussian plus some constant term:

$$F = C + \frac{1}{\sqrt{2\pi\sigma}} e^{\frac{(x-x_0)^2}{2\sigma^2}} \tag{1}$$

one can find backgrounds in center and outer pads normalized to the N=1 flux and study their behavior versus Ecal position. The ratio of two is the measure of nonuniformity of the background.

Figure 2 shows an example of normalized Ecal signals for 4 top rows of Ecal plotted versus X-position of the laser focus. Each plot shows central pads (closed circles) and outer pads (open circles); the ratio of the center to the outer pads (ratio of constants C from equation 1) is indicated.

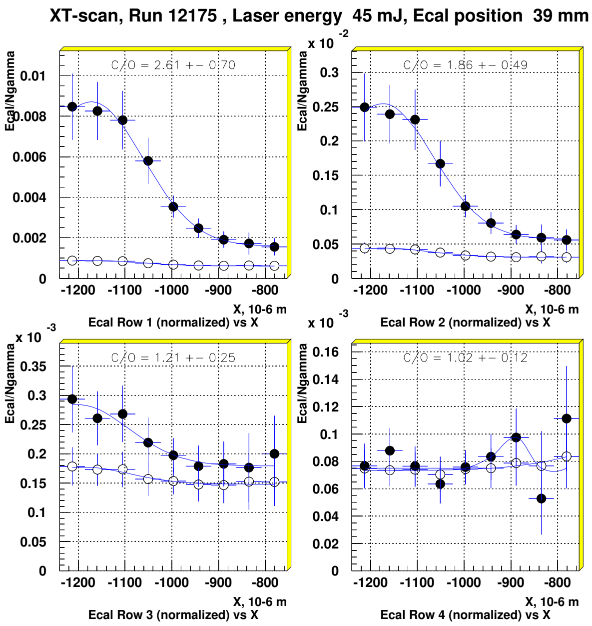

FIG. 2. Example of different backgrounds for center and outer pads for XT-scan 12175. Ecal central pad (solid circles) and outer pad (open circles) signals are normalized to N=1 signal and plotted versus X-position of the laser IP box and therefore of the laser focal point. Four plots correspond to four top rows of Ecal; ratios of central to outer pad signals out of focus are also shown with corresponding errors.

Horizontal axis is the X-position of the laser focus in μm. Vertical axis is the signal in Ecal in GeV normalized to the γ-flux (per 10^4 γ's).

A total of about 25 XT-scans were taken during March95 Run with two laser wavelengths both linear and circular polarization. Most IR laser runs had a 12mm W-plate on top of Ecal that served as shielding for Ecal from the background. During green laser operation this plate was removed. Tables I and II present results from XT-scans for most of these 25 runs (for the rest of them results were not reliable either because run had only 4-5 points or because they were not completed). Table I contain backgrounds in four top rows of Ecal for center pads in GeV per 10^4 γ. Backgrounds and errors correspond to the parameter C from the fit of distributions by the function (1).

Run	Pos mm	Laser energy	Row 1 GeV	Row 2 GeV	Row 3 GeV	Row 4 GeV	Laser; Polarization; Shielding on top
12116	28	18 mJ	15.20±1.48	1.46±.22	.38±.04	.09±.05	IR; Circular; NO plate
12164	38	18 mJ	15.49±4.01	5.37±1.72	2.11±.16	.76±.10	IR; Circular; Plate
12175	39	45 mJ	15.87±3.50	5.70±1.18	1.80±.28	.75±.06	-
12205	62	126 mJ	2.83±1.02	1.02±.28	.54±.09	.36±.02	-
12250	71	243 mJ	1.99±.23	.81±.10	.42±.10	.31±.01	-
12257	79	311 mJ	1.70±.15	.69±.05	.38±.04	.25±.01	-
12297	95	443 mJ	1.24±.15	.56±.01	.30±.02	.18±.01	IR; Linear; Plate
12338	97	930 mJ	1.22±.10	.51±.04	.28±.03	.17±.01	IR; Circular; Plate
12351	112	722 mJ	1.08±.03	.44±.01	.23±.01	.14±.01	-
12388	82	12 mJ	4.51±.72	2.18±.51	.65±.35	-.26±.07	GREEN; Circular; NO plate
12411	81	123 mJ	7.83±.92	4.85±.57	1.42±.17	.15±.02	-
12419	114	200 mJ	.78±.17	.13±.01	.05±.01	.03±.01	-
12430	113	255 mJ	1.54±.21	.20±.02	.09±.01	.03±.01	-
12445	81	30 mJ	3.79±.64	2.13±.37	.70±.11	.15±.01	GREEN; Linear; NO plate
12474	82	13 mJ	5.63±.60	2.51±.34	1.16±.16	.27±.02	-

TABLE I. *Background in the Center Pads of Ecal for some XT-scans. Background (GeV) is per 10^4 γ measured by N=1 monitor.*

Table II has the ratio of the backgrounds in center and outer pads for the same runs.

Run	Pos mm	Row 1 C/O	Row 2 C/O	Row 3 C/O	Row 4 C/O	Laser; Polarization; Shielding on top
12116	28	1.87±.21	1.54±.27	1.14±.17	.71±.37	IR; Circular; NO plate
12164	38	2.21±.62	1.55±.54	1.30±.13	1.00±.17	IR; Circular; Plate
12175	39	2.61±.70	1.86±.49	1.21±.24	1.02±.12	-
12205	62	1.46±.61	1.12±.39	1.04±.24	1.04±.07	-
12250	71	1.45±.54	1.38±.78	.90±.21	1.05±.05	-
12257	79	1.15±.13	1.03±.10	1.07±.52	1.05±.05	-
12297	95	1.02±.13	1.03±.05	1.06±.08	1.02±.08	IR; Linear; Plate
12338	97	1.02±.09	.97±.08	1.04±.12	1.02±.05	IR; Circular; Plate
12351	112	1.06±.05	1.00±.04	1.03±.04	1.00±.04	-
12388	82	2.35±.39	2.53±.62	1.52±.83	-	GREEN; Circular; NO plate
12411	81	6.14±.90	7.32±1.09	4.78±.70	1.37±.19	-
12419	114	3.40±.83	1.30±.22	.91±.09	1.10±.08	-
12430	113	5.39±.98	1.49±.23	1.33±.17	.98±.10	-
12445	81	3.92±.77	3.52±.64	2.60±.44	1.01±.22	GREEN; Linear; NO plate
12474	82	2.42±.28	2.38±.37	1.70 ±.26	2.36±1.05	-

TABLE II. *Background Ratio Center/Outer pads for some XT-scans*

The same data plotted in graphical form are presented in Figs 3, 4,5 and 6.

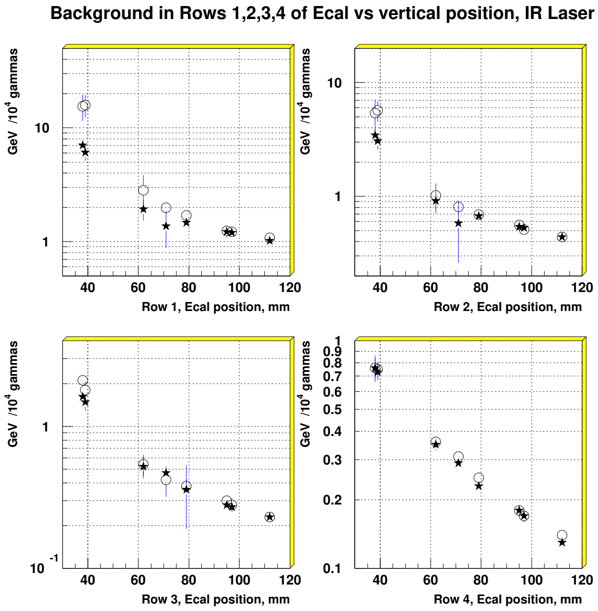

FIG. 3. Background for central pads (open circles) and outer pads (stars) for 4 rows of Ecal vs Ecal position for IR-laser runs. Background (GeV) is normalized to the γ-flux of 10^4 γ.

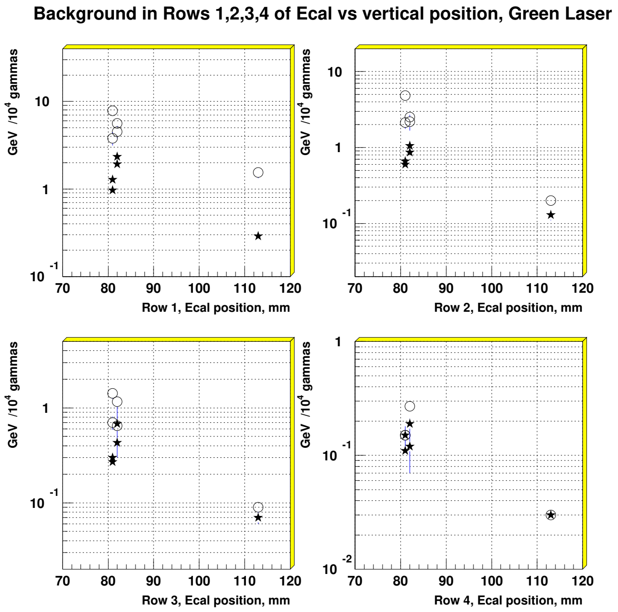

FIG. 4. Background for central pads (open circles) and outer pads (stars) for 4 rows of Ecal vs Ecal position for GREEN-laser runs. Background (GeV) is normalized to the γ-flux of 10^4 γ.

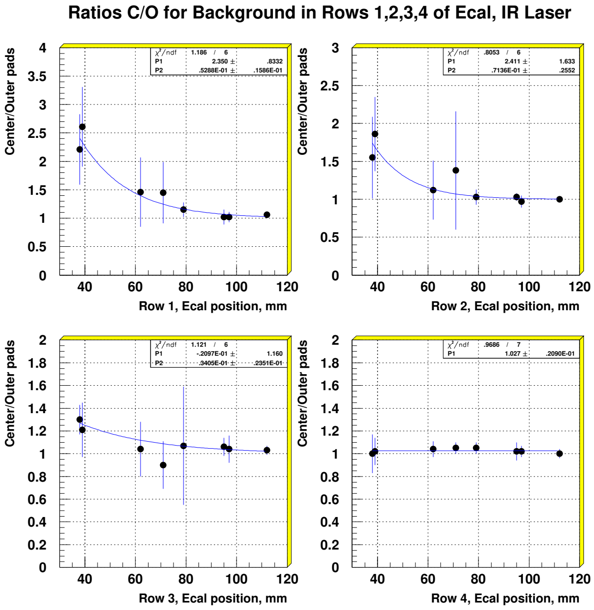

FIG. 5. Ratio of the backgrounds Center/Outer pads vs Ecal position for IR laser runs. Results of the fit by function R(y) (see the text) are also shown.

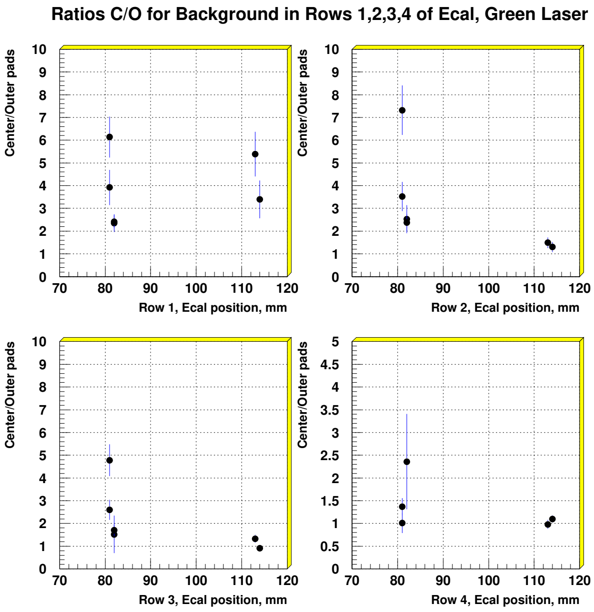

FIG. 6. Ratio of the backgrounds Center/Outer pads vs Ecal position for GREEN laser runs.

One can notice that the background in the center pads and outer pads became almost equal for low Ecal positions. This naturally suggest that the ratio of two backgrounds should go asymptotically to 1 - background became uniform for low Ecal positions. Figures 5 have a fit by function:

$$R(y) = 1 + e^{p_1 - y\,p_2} \tag{2}$$

which asymptotically approaches 1.

III. DISCUSSION OF THE RESULTS

First, let us note that the N=1 background analyzed above doesn't have contribution from the plural N=1 scattering of an electron in the laser field. This can be noticed by comparing XT-runs with the same Ecal position and different laser energies. Normalized background in central pads (Table I) doesn't depend on laser intensity (for instance IR runs 12164 and 12175, 12297 and 12338 with the same Ecal position). Recall that two-step N=1 process is proportional to the square of laser intensity; normalized two-step process should be proportional to the laser intensity.

There is no effect of laser polarization on backgrounds (IR runs 12297 and 12338, Green runs 12388 and 12445).

Shielding on top of Ecal seems doesn't improve the situation with backgrounds. Though we have the only IR run 12116 without shielding (in this analysis) it shows significantly lower backgrounds especially in rows 3 and 4 of Ecal.

Though Green data has higher normalized backgrounds in the top row for the same Ecal positions (compare runs IR-12257 and Green-12411) it has background decreasing rapidly for rows 2 to 4. It could be explained by different spectrum of N=1 electrons for Green laser but also fast decreasing backgrounds can be attributed due to the absence of shielding on top of Ecal.

Nonuniformity of the background (ratio of the center to outer pads) decreases (goes to 1) for low Ecal positions (Ecal is further from the path of scattered electrons).

For IR runs one can see from the plot 5 that statistically significant nonuniformity of the background can be seen only in rows 1 and 2 of Ecal for high Ecal positions. For row 3 though there is an indication of a slightly nonuniform background at the high Ecal position the constant fit ($R = 1$) to the data has χ^2 not significantly different from χ^2 from the exponent fit (2). For row 4 there is no any indication of nonuniform backgrounds.

Green laser runs (Fig. 6) seems to have significantly more background in the center pads than in the outer one for Ecal position 81-82 mm. In this position Ecal was located close to N=1 edge in electron spectrum. There are only 2 positions for XT-scans for Green laser and it is difficult to draw firm conclusions. Still one suggestion is urgent: **there is a danger of overestimating the N=2 signal for high Ecal position (low laser intensity)** because there is much more background in the center pads compared to the outer pads for this runs.

To find background in GeV one must multiply normalized background in Ecal by the γ-flux. This flux is different for different Ecal positions. Because of the limited dynamic range of Ecal the calorimeter was positioned lower for high laser intensities than for lower laser intensities. There is a correlation between typical γ flux (and hence the background) and Ecal position in the data runs because of the data taking strategy. This dependence for all data runs is presented on Fig. 7 separately for IR and Green laser polarization.

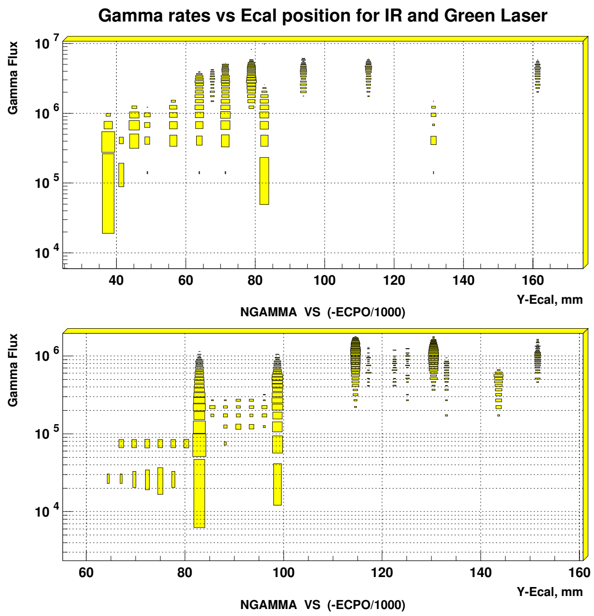

FIG. 7. Flux of γ versus Ecal position for IR and Green laser. All Data runs used in the analysis of the nonlinear Compton signal in Ecal are represented.

One can compare also the **reconstructed signal** in Ecal compared to the **reconstructed** background. Reconstruction of the signal and background takes into account shower leakage between different rows and between center and outer pads of Ecal and is described elsewhere. Two plots, Fig. 8 and Fig. 9 show backgrounds in Ecal compared to the signal for IR and Green laser runs.

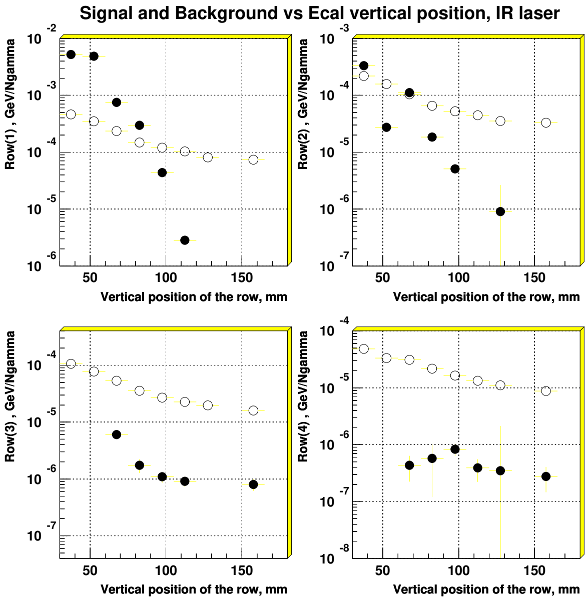

FIG. 8. Reconstructed signal (solid circles) and background (open circles) for all IR laser data runs. Signal and background are normalized to the number of photons - GeV/Nγ. 4 plots corresponds to 4 rows of Ecal. Some points for the signal (in rows 3 and 4) are not shown because reconstruction failed for these points and gave negative numbers.

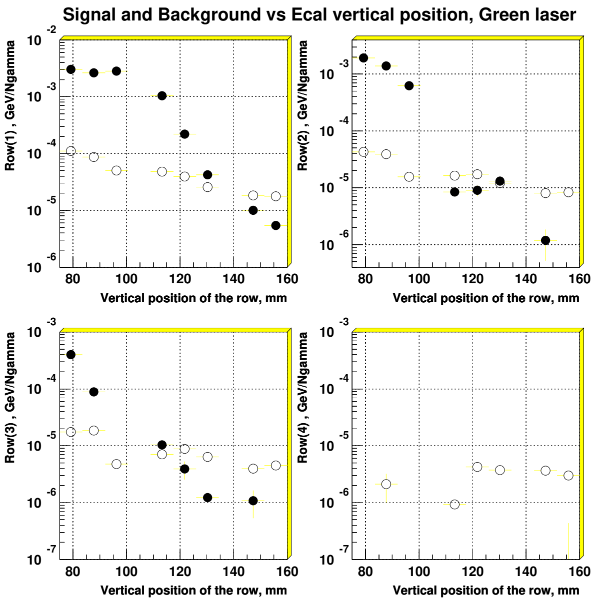

FIG. 9. Reconstructed signal (closed circles) and background (open circles) for all GREEN laser data runs. Signal and background are normalized to the number of photons - GeV/Nγ. 4 plots corresponds to 4 rows of Ecal. Some points for the signal (in row 4) are not shown because reconstruction failed for these points and gave negative numbers.

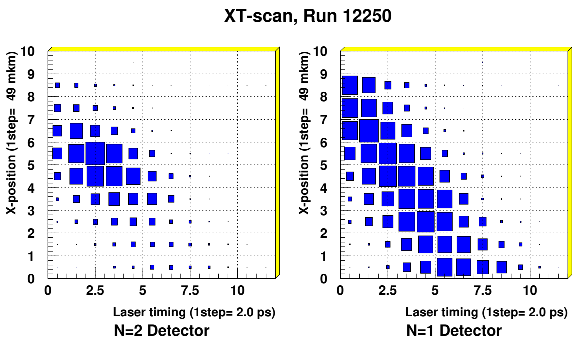

FIG. 10. N=2 and N=1 signals during XT-scan, Run 12250

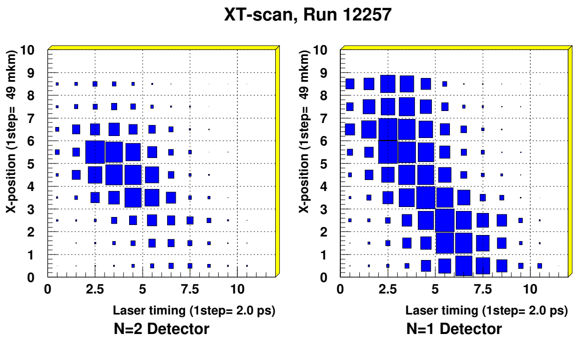

FIG. 11. N=2 and N=1 signals during XT-scan, Run 12257

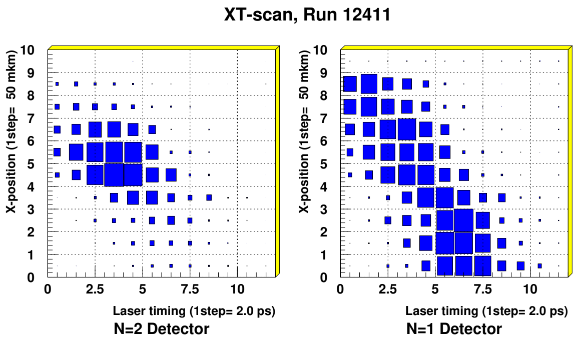

FIG. 12. N=2 and N=1 signals during XT-scan, Run 12411

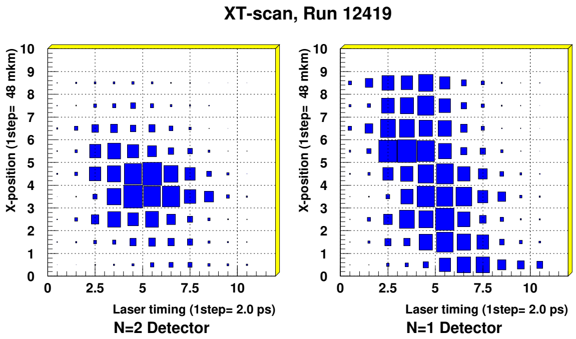

FIG. 13. N=2 and N=1 signals during XT-scan, Run 12419

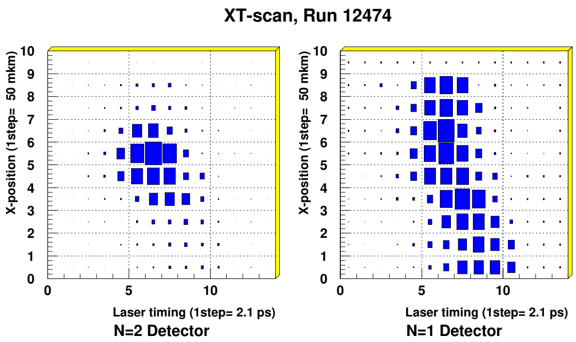

FIG. 14. N=2 and N=1 signals during XT-scan, Run 12474

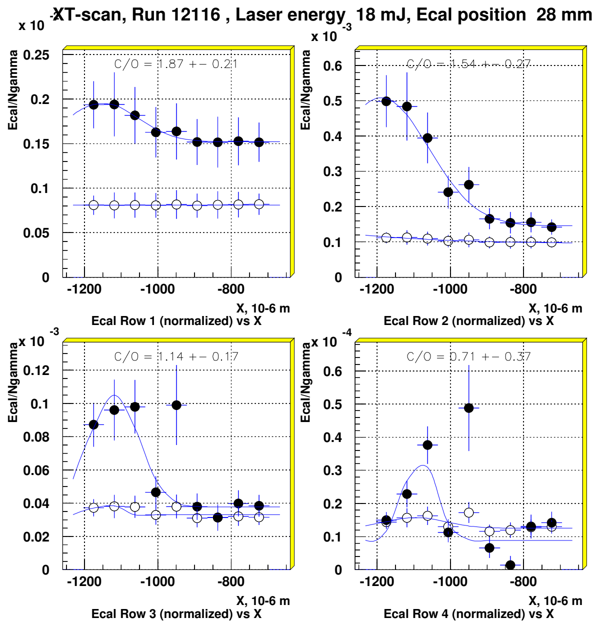

FIG. 15. Center and outer pads signal of ECAL during XT-scan, Run 12116

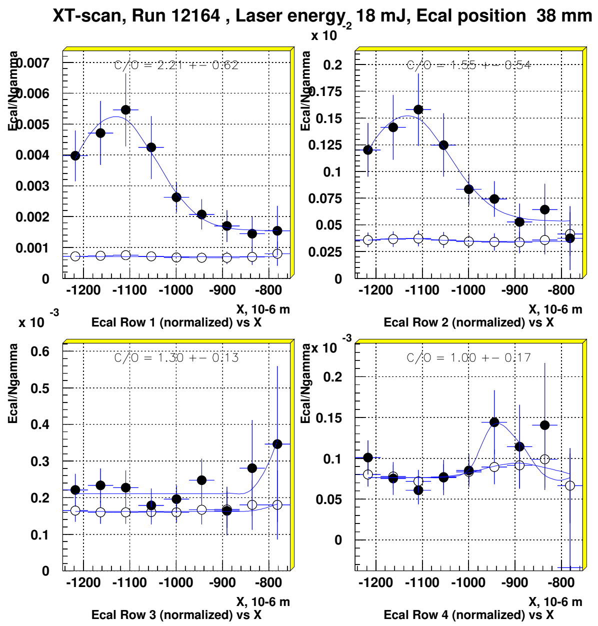

FIG. 16. Center and outer pads signal of ECAL during XT-scan, Run 12164

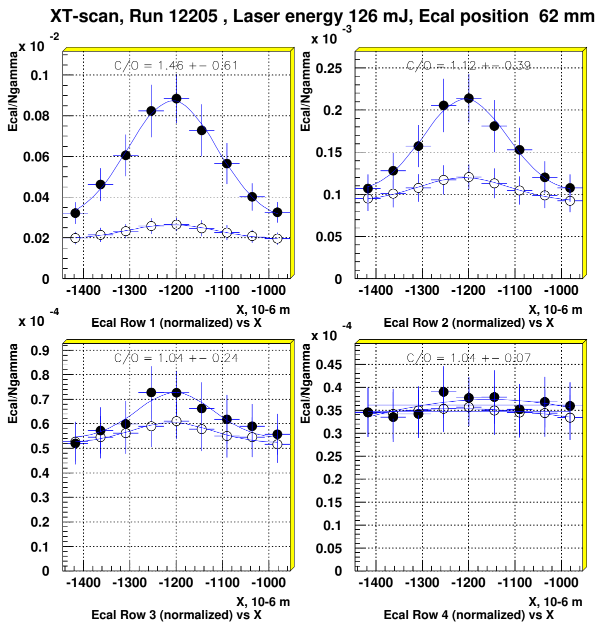

FIG. 17. Center and outer pads signal of ECAL during XT-scan, Run 12205

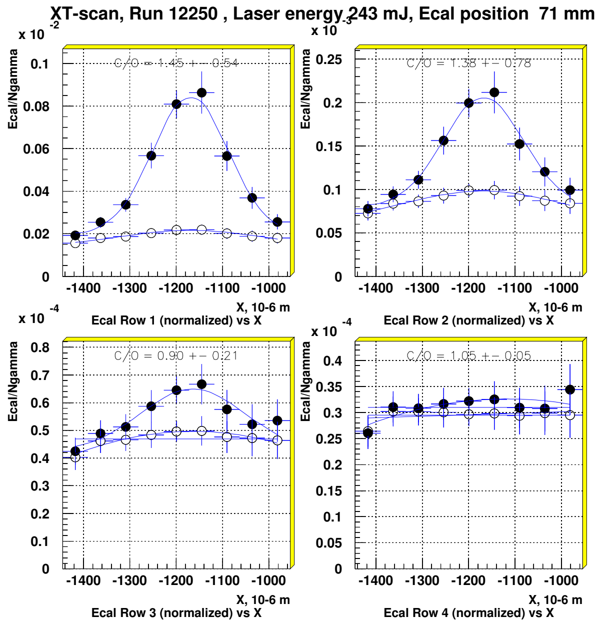

FIG. 18. Center and outer pads signal of ECAL during XT-scan, Run 12250

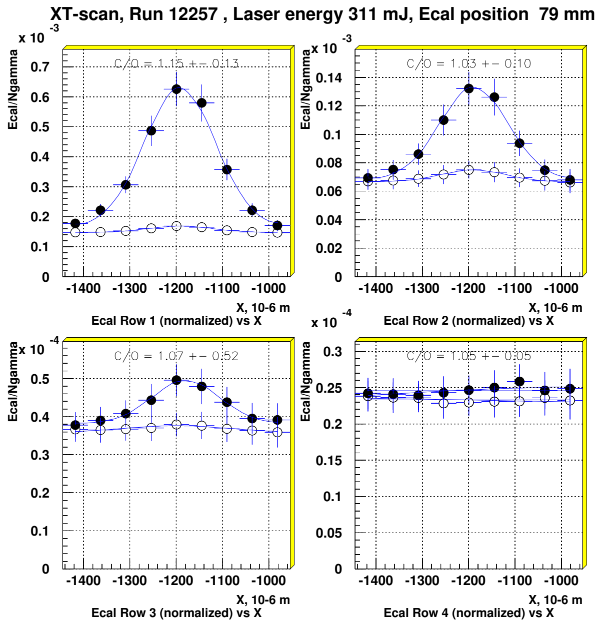

FIG. 19. Center and outer pads signal of ECAL during XT-scan, Run 12257

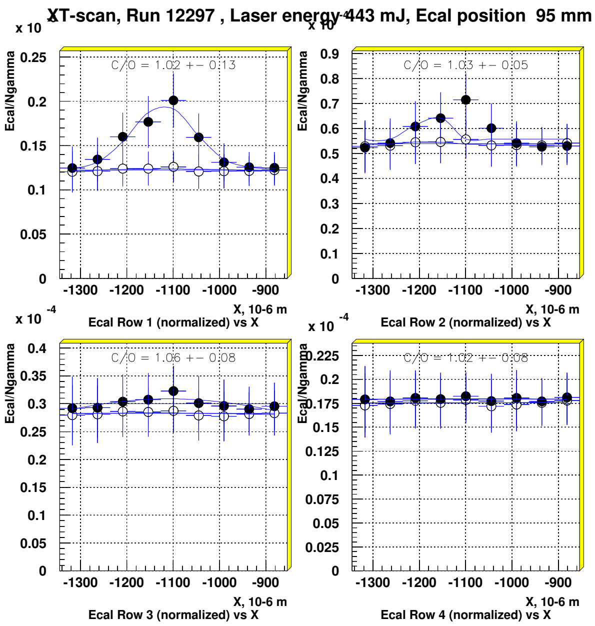

FIG. 20. Center and outer pads signal of ECAL during XT-scan, Run 12297

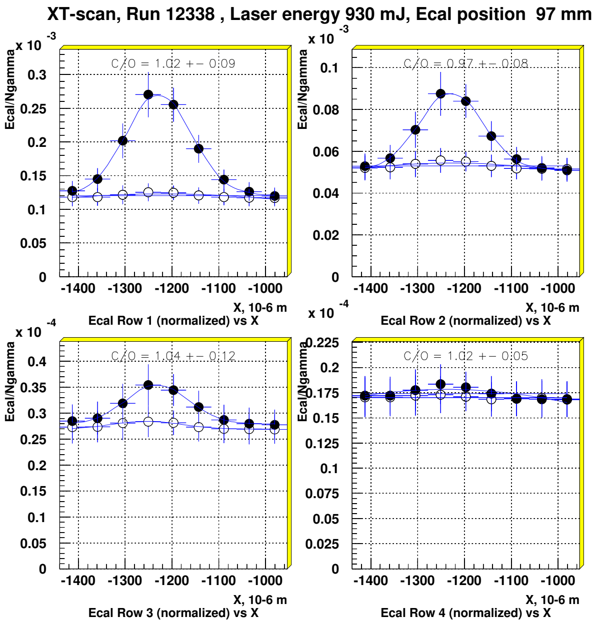

FIG. 21. Center and outer pads signal of ECAL during XT-scan, Run 12338

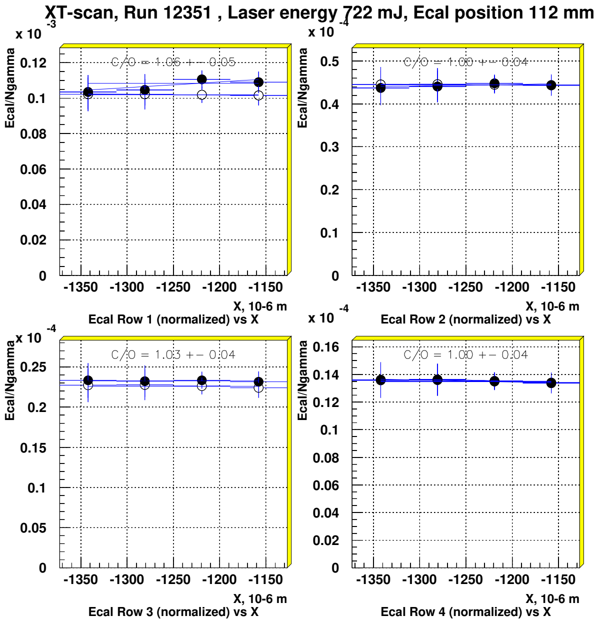

FIG. 22. Center and outer pads signal of ECAL during XT-scan, Run 12351

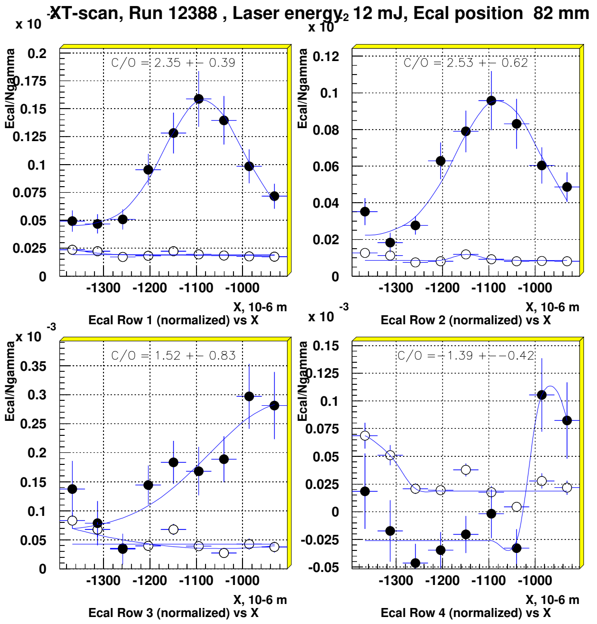

FIG. 23. Center and outer pads signal of ECAL during XT-scan, Run 12388

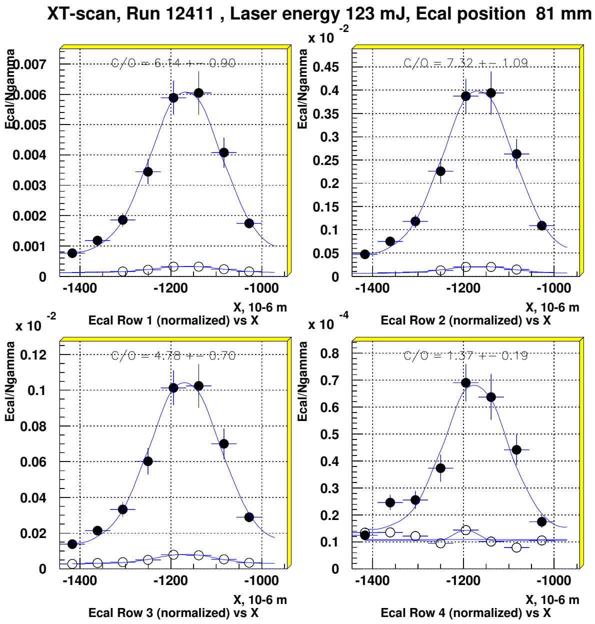

FIG. 24. Center and outer pads signal of ECAL during XT-scan, Run 12411

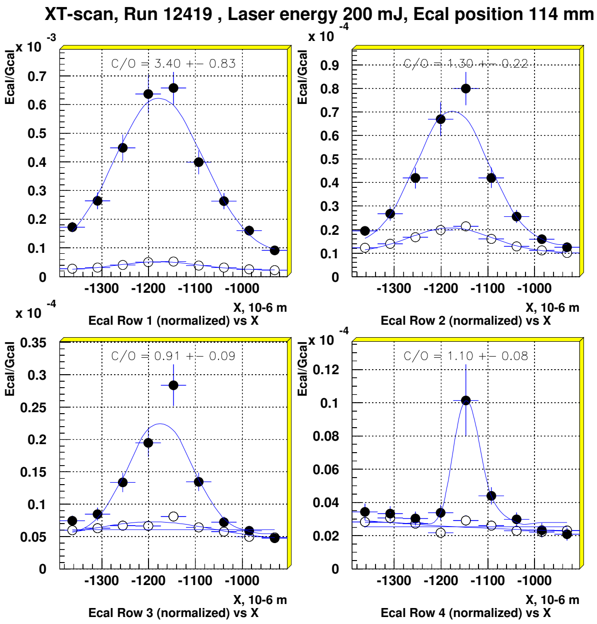

FIG. 25. Center and outer pads signal of ECAL during XT-scan, Run 12419

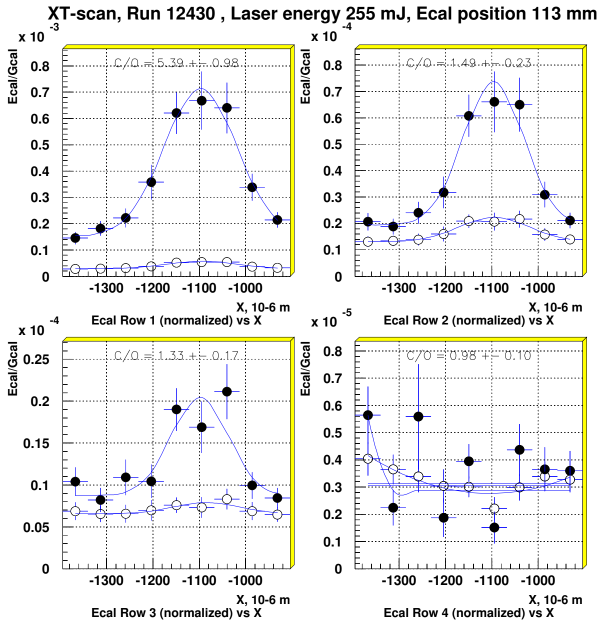

FIG. 26. Center and outer pads signal of ECAL during XT-scan, Run 12430

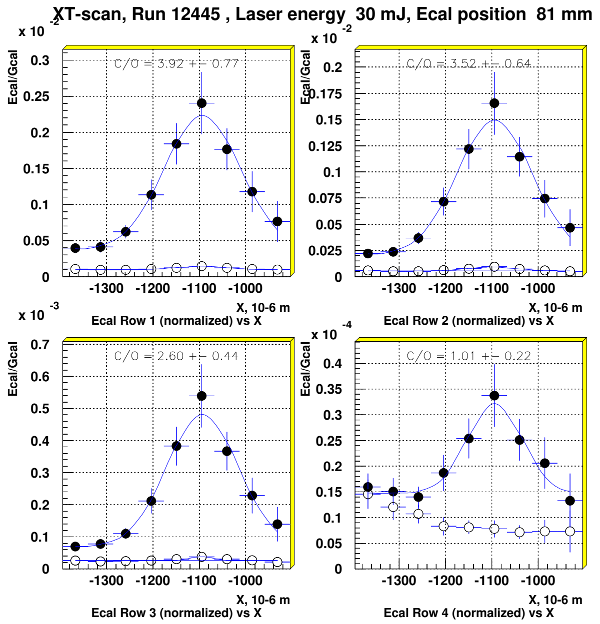

FIG. 27. Center and outer pads signal of ECAL during XT-scan, Run 12445

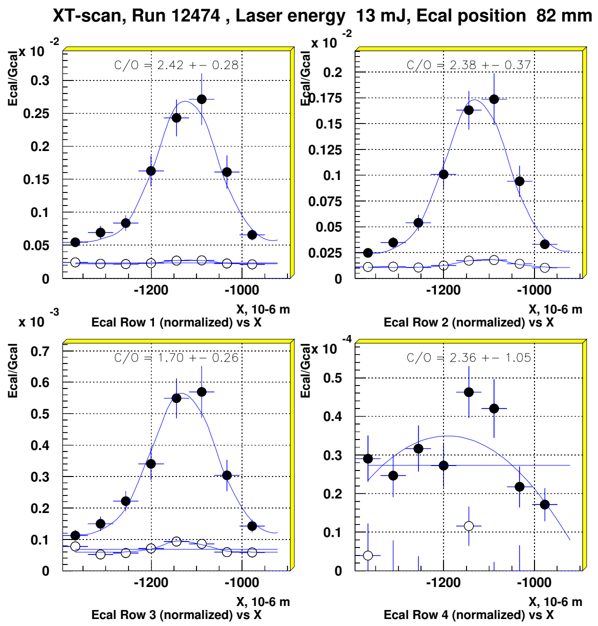

FIG. 28. Center and outer pads signal of ECAL during XT-scan, Run 12474